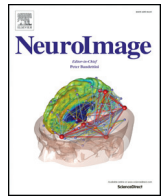




Contents lists available at ScienceDirect

NeuroImage

journal homepage: www.elsevier.com/locate/ynimg

Q1 New tissue priors for improved automated classification of subcortical brain structures on MRI☆

Q2 S. Lorio^a, S. Fresard^a, S. Adaszewski^a, F. Kherif^a, R. Chowdhury^c, R.S. Frackowiak^a, J. Ashburner^c, G. Helms^b,
N. Weiskopf^{c,d}, A. Lutti^{a,1}, B. Draganski^{a,d,*}

^a LREN, Department of Clinical Neurosciences, CHUV, University of Lausanne, Lausanne, Switzerland

^b Medical Radiation Physics, Lund University Hospital, Lund, Sweden

^c Wellcome Trust Centre for Neuroimaging, UCL Institute of Neurology, London, UK

^d Max Planck Institute for Human Cognitive and Brain Sciences, Leipzig, Germany

1 0 A R T I C L E I N F O

Article history:

Received 28 October 2015

Accepted 29 January 2016

Available online xxx

Keywords:

Relaxometry

Magnetization transfer saturation

Effective transverse relaxation

Basal ganglia

Tissue probability maps

Voxel-based morphometry

Voxel-based quantification

A B S T R A C T

Despite the constant improvement of algorithms for automated brain tissue classification, the accurate delineation of subcortical structures using magnetic resonance images (MRI) data remains challenging. The main difficulties arise from the low gray-white matter contrast of iron rich areas in T1-weighted (T1w) MRI data and from the lack of adequate priors for basal ganglia and thalamus. The most recent attempts to obtain such priors were based on cohorts with limited size that included subjects in a narrow age range, failing to account for age-related gray-white matter contrast changes. Aiming to improve the anatomical plausibility of automated brain tissue classification from T1w data, we have created new tissue probability maps for subcortical gray matter regions. Supported by atlas-derived spatial information, raters manually labeled subcortical structures in a cohort of healthy subjects using magnetization transfer saturation and R2* MRI maps, which feature optimal gray-white matter contrast in these areas. After assessment of inter-rater variability, the new tissue priors were tested on T1w data within the framework of voxel-based morphometry. The automated detection of gray matter in subcortical areas with our new probability maps was more anatomically plausible compared to the one derived with currently available priors. We provide evidence that the improved delineation compensates age-related bias in the segmentation of iron rich subcortical regions. The new tissue priors, allowing robust detection of basal ganglia and thalamus, have the potential to enhance the sensitivity of voxel-based morphometry in both healthy and diseased brains.

© 2016 Published by Elsevier Inc.

Introduction

Computer-based assessment of brain anatomy with magnetic resonance imaging (MRI) has become a powerful method to investigate *in vivo* the healthy and diseased brain. Aiming to provide reliable estimates of local gray matter (GM) volume across the whole brain, a substantial amount of work has been devoted to the improvement of the accuracy of algorithms for automated tissue classification and spatial registration (Ashburner and Friston, 2000, 2005; Klein et al., 2010). Despite major methodological advances, the robust and accurate delineation of the deep brain nuclei – thalamus, caudate, putamen, pallidum, subthalamic nucleus, substantia nigra, and red nucleus – remains challenging (Lim et al., 2013; Streitbürger et al., 2014;

Callaert et al., 2014). The basal ganglia play a crucial role in goal-directed behavior and movement control, which explains their involvement in many neurological and neuropsychiatric disorders such as Parkinson's and Huntington's disease, dystonia, tremor, Tourette's syndrome, and schizophrenia (Utter and Basso, 2008). The reliable anatomical assessment of these regions is important not only to accurately monitor disease-related changes but also to facilitate accurate target identification for functional neurosurgery in basal ganglia disorders. There is therefore a clear need to improve the automated detection of basal ganglia structures (Ahsan et al., 2007).

Automated tissue classification relies on the distributions of image intensities and gray-white matter contrast in MRI images (Ashburner et al., 2003), which are determined by the local values of the MRI parameters and the microstructural composition of brain tissue (Fukunaga et al., 2010; Streitbürger et al., 2014; Lutti et al., 2014). In particular, the inaccurate classification of subcortical structures from T1-weighted (T1w) images—the most widely used data in computational anatomy, arises from the high concentration of iron in these regions (Hallgren and Sourander, 1958; Haacke et al., 2005; Lorio

☆ Disclosure: The Wellcome Trust Centre for Neuroimaging receives support from Siemens Healthcare.

* Corresponding author at: LREN, Department of Clinical Neurosciences, CHUV, University of Lausanne, Lausanne, Switzerland. Fax: +41 21 314 12 56.

E-mail address: bogdan.draganski@chuv.ch (B. Draganski).

¹ Equal contribution.

et al., 2014). Importantly, this effect is further modulated by age-related tissue property changes (Lorio et al., 2014).

In addition to its dependence on image intensity and gray-white matter contrast, the automated tissue classification relies on prior spatial information based either on stereotaxic atlases (Fischl et al., 2002; Pohl et al., 2006; Khan et al., 2008) or on probabilistic maps of tissue class distributions derived from MRI data (Ashburner and Friston, 2005). The currently used tissue probability maps are based on T1w data (Mazziotta et al., 2001) with the major drawback of a regional contrast differences driven by microstructural tissue properties (Lorio et al., 2014). More recent attempts to improve the priors for robust classification of subcortical structures have benefited from new MRI protocols that highlight the impact of tissue properties on gray-white matter contrast. These recent achievements are limited by the relatively low number of used data samples, which hampers the accurate detection of inter-individual variations in brain anatomy and their modulation by age (Ahsan et al., 2007; Prodoehl et al., 2008; Lim et al., 2013; Keuken et al., 2014). Common to the previous studies on the topic is that there was no attempt to statistically assess the impact of new anatomically plausible tissue probability maps on the automated tissue classification within computational anatomy frameworks.

The purpose of this study is to build new tissue probability maps (TPMs) for the automated tissue classification of thalamus, caudate, putamen, globus pallidus, substantia nigra, subthalamic nucleus, red nucleus, and cerebellar dentate. The new TPMs were derived from the manual labeling of subcortical structures on magnetization transfer saturation (MT) and $R2^*$ ($= 1/T2^*$) maps, which provide optimal contrast in these areas (Helms et al., 2009). The obtained TPMs were then included as a new tissue prior in the Bayesian framework for tissue classification of the well-established SPM software (Ashburner and Friston, 2005). To test the anatomical accuracy of the tissue classification performed with the new TPMs, we carried out a cross-validation between the manual labeling results and the gray matter volume maps obtained from the automated tissue classification based on MT images. Finally, the new TPMs were applied on an independent data set of T1w images. Our hypothesis was that the new tissue probability maps would enable the accurate delineation of subcortical structures and would prove particularly robust against the effects of age-related microstructural tissue changes on T1w data.

Methods

Data acquisition

We used quantitative MRI (qMRI) data for the manual labeling of subcortical structures. The qMRI images were originally acquired for

previous studies (Chowdhury et al., 2013; Lorio et al., 2014). The data set comprised 96 healthy adults (40 male, age range 27–74 years, mean 55 ± 15 ; 56 female, age range 21–88 years, mean 57 ± 19) scanned on a 3 T whole-body MRI system (Magnetom TIM Trio, Siemens Medical Systems, Germany), using a standard 32-channel radio-frequency receive head coil and body coil for transmission. On visual inspection, study participants showed neither macroscopic brain abnormalities, i.e., major atrophy, nor signs of overt vascular pathology, i.e., micro-bleeds and white matter lesions. Elderly subjects with white matter lesions of Grade 2 or more by the Scheltens' rating scale (Scheltens et al., 1993; Wardlaw et al., 2013) were excluded from the study. We obtained quantitative measures of brain atrophy by calculating the brain volume fraction (Rudick et al., 1999) from MT images.

The quantitative MRI acquisitions consisted of three multi-echo 3D fast low angle shot (FLASH) acquired with predominant proton density, PD-, T1-, and MT-weighting (PD-weighted: $TR/\alpha = 23.7 \text{ ms}/6^\circ$; T1-weighted: $TR/\alpha = 18.7 \text{ ms}/20^\circ$; MT-weighted: $TR/\alpha = 23.7 \text{ ms}/6^\circ$) with 1 mm^3 isotropic resolution (Helms et al., 2008a; Weiskopf et al., 2013). The MT-weighting was achieved by applying an off-resonance Gaussian-shaped pulse (4 ms duration, 220 nominal flip angle, 2 kHz frequency offset from water resonance) prior to the excitation. Multiple gradient echoes were acquired for each FLASH acquisition with alternating readout polarity: 6 equidistant echo time (TE) were used for the T1- and MT-weighted sets (TE between 2.34 ms and 14.7 ms) and 8 equidistant TE were used for PD-weighted sets (TE between 2.34 ms and 19.7 ms). The image resolution was 1 mm isotropic. To shorten the acquisition time, parallel imaging (acceleration factor 2, GRAPPA), and partial Fourier acquisition were used. To correct the quantitative maps for the effect of RF transmit inhomogeneities, we measured the transmit field $B_1 +$ using 3D echo-planar imaging (EPI) spin-echo (SE) and stimulated echo (STE) images. The EPI images were acquired with the 4 mm isotropic resolution, parallel imaging using GRAPPA factor 2×2 in PE and partition direction, TESE/TESTE/TM (mixing time)/ $TR = 37.06/37.06/31.2/500 \text{ ms}$. A B_0 map was acquired to correct the RF transmit field maps for geometric distortion and off-resonance effects. The acquisition protocol used a 2D double-echo FLASH sequence with the following parameters (Lutti et al., 2012, 2010): slice thickness = 2 mm, $TR = 1020 \text{ ms}$, $TE_1/TE_2 = 10/12.46 \text{ ms}$, $\alpha = 90^\circ$, $BW = 260 \text{ Hz/pixel}$ and flow compensation. The total acquisition time was 24 min (for details on MRI acquisition parameters see Table 1, Supplementary material).

Quantitative MRI maps were calculated from the acquired data using an in-house code running under SPM12 (Wellcome Trust Centre for Neuroimaging, London, UK; <http://www.fil.ion.ucl.ac.uk/spm>) and Matlab 7.11 (Mathworks, Sherborn, MA, USA). The $R2^*$ maps were

Table 1
Manual labeling results. Subcortical structures' mean volume, global percentage of voxels not included by all raters (disagreement voxels), and inter-rater agreement indices (Dice index, Cohen's kappa, and intraclass coefficient (ICC)). RN = red nucleus; STN = subthalamic nucleus; SN = substantia nigra; GP = globus pallidus.

Structure	Volume (mm^3)		% of disagreement voxels		Dice index		Cohen's kappa		ICC		
	Mean	SD	Mean	SD	Mean	SD	Mean	SD	Mean	SD	
Caudate	Left	3421	900	17	3	0.83	0.06	0.85	0.06	0.83	0.06
	Right	3306	700	16	3	0.85	0.06	0.86	0.06	0.85	0.06
Putamen	Left	3906	650	19	3	0.80	0.05	0.8	0.05	0.83	0.05
	Right	3966	690	18	4	0.85	0.03	0.86	0.03	0.84	0.04
GP	Left	1319	235	20	4	0.79	0.08	0.8	0.08	0.78	0.08
	Right	1263	201	21	5	0.76	0.09	0.77	0.09	0.77	0.09
Thalamus	Left	5110	1100	16	4	0.86	0.04	0.86	0.04	0.86	0.04
	Right	5495	1301	15	3	0.87	0.05	0.87	0.05	0.87	0.04
SN	Left	330	94	25	6	0.7	0.11	0.74	0.12	0.67	0.11
	Right	330	90	23	5	0.76	0.14	0.77	0.14	0.68	0.12
RN	Left	220	49	29	7	0.68	0.13	0.71	0.13	0.64	0.1
	Right	220	50	28	8	0.69	0.11	0.77	0.11	0.67	0.11
STN	Left	86	28	33	7	0.65	0.14	0.70	0.12	0.67	0.1
	Right	85	20	31	7	0.7	0.1	0.73	0.19	0.69	0.1
Dentate	Left	1032	215	20	5	0.76	0.11	0.73	0.11	0.7	0.11
	Right	1013	195	23	6	0.77	0.14	0.76	0.13	0.69	0.12

Download English Version:

<https://daneshyari.com/en/article/6023664>

Download Persian Version:

<https://daneshyari.com/article/6023664>

[Daneshyari.com](https://daneshyari.com)